

Title: Mechanisms of Host Cell Binding and Neurotropism of Zika Virus

C.A. Rieder¹, J. Rieder¹, S. Sannajust^{1,2}, D. Goode^{1,2}, R. Geguchadze^{1,2}, R.F. Relich³, D.C. Molliver^{1,2}, T.E. King^{1,2}, J. Vaughn¹, M. May^{1,2*}

¹Department of Biomedical Sciences, College of Osteopathic Medicine, University of New England

²Center for Excellence in the Neurosciences, University of New England

³Department of Pathology and Laboratory Medicine, Indiana University School of Medicine

Material Requests and Correspondence should be addressed to:

Meghan May

11 Hills Beach Road, 423 Stella Maris Hall, Biddeford, ME USA 04005

mmay3@une.edu

Keywords: Zika Virus, Neurotropism, Microcephaly, ASN154, N-acetylglucosamine, Encephalitis, Guillan-Barre syndrome, binding motif

Abstract:

Zika virus (ZIKV) recently emerged in the Western Hemisphere with previously unrecognized or unreported clinical presentations. Here, we identify two distinct binding mechanisms of ancestral and emergent ZIKV strains featuring the envelope (E) protein residue ASN154 and viral phosphatidylserine (PS). Short (20-mer) peptides representing the region containing ASN154 from strains PRVABC59 (Puerto Rico 2015) and MR_766 (Uganda 1947) were exposed to neuronal cells and fibroblasts, expecting interactions to be representative of ZIKV E protein/cell interactions, and bound MDCK or Vero cells and primary neurons significantly above a scrambled PRVABC59 control peptide. Peptides also significantly inhibited Vero cell adsorption by ZIKV strains MR_766 and PRVABC59, indicating that we have identified a binding mechanism of ancestral African ZIKV strains and emergent Western Hemisphere strains. Pretreatment of ZIKV MR_766 and PRVABC59 with the PS-binding protein annexin V significantly inhibited replication of PRVABC59, but not MR_766, suggesting that Western hemisphere strains are additionally utilizing PS-mediated entry to infect host cells. Taken together, these data indicate that we have identified an ancestral binding mechanism of ZIKV, and a secondary binding mechanism utilized by Western Hemisphere strains.

Background

Zika virus (ZIKV) is a mosquito-borne *Flavivirus* that recently emerged and established endemicity in the Western Hemisphere (reviewed here¹⁻²). ZIKV disease historically presented as a mild febrile illness featuring myalgia, rash, and conjunctivitis; however, novel and more severe clinical presentations and increased disease incidence were reported as the virus emerged in the South Pacific³⁻⁴ and the Western Hemisphere⁵⁻⁷. Since that time, case reports and animal models have implicated ZIKV in a congenital syndrome most notably featuring microcephaly⁷⁻¹², primary encephalitis, encephalomyelitis, lysencephaly, or Guillan-Barré syndrome^{5, 13-20}, chorioamnionitis²¹, testicular infection²², changes in semen quality²³, and potentially a hemorrhagic shock syndrome²⁴⁻²⁵. The biology and pathogenesis of ZIKV were virtually unexplored at the time of its detection in the Western Hemisphere, making rapid progress toward diagnostics, therapeutics, or vaccine development challenging in the absence of targets²⁶.

Substantial progress in the understanding of ZIKV biology has been made in a short time, and includes identification of divergent nucleotide and amino acid sites²⁷⁻³⁰, potential host cell ligands³¹⁻³³, factors that impact replication kinetics³⁴⁻³⁷, and the development of animal models for both neurological and prenatal disease³⁸⁻³⁹. A recent study by Yuan *et al.* demonstrated that a single amino acid substitution within the PrM protein of Western Hemisphere strains conferred increased virulence and resulted in exacerbated pathology *in vivo*³⁷. While this change confers an increased capacity for cell death and correlates with the clinical findings suggesting more severe and invasive disease, it cannot explain the newly emerged ability to directly invade the central nervous system (CNS). We sought to build upon our recent informatics analysis²⁷ by utilizing the findings to identify the binding mechanism of

ZIKV. We hypothesized that NAG-glycosylation of E protein ASN154 is linked to ZIKV neuroinvasiveness and that this region plays a critical role in host cell adsorption across strains.

Results and Discussion

Binding Motif Prediction

Structural modeling predictions of strain PRVABC59 (Puerto Rico, 2015) indicated that ASN154 is part of a linear β strand (Fig.1A). The disorder probability of this region peaks at 0.72 (Fig.1B), suggesting that this portion of the E protein is particularly dynamic and flexible. Structural and disorder probability predictions of the African type strain MR_766 (Uganda 1947) and the Nigerian strain IbH30656 (Nigeria, 1968) exhibit similar characteristics (Fig.1C, D). This region was termed the (putative) Zika virus binding motif (ZVBM).

ZVBM Binding and ZIKV Inhibition

ZVBM sequences from strains PRVABC59, MR_766, and IbH30656 were synthesized and N-terminally labelled with fluorescein isothiocyanate (FITC) (Table 1) in order to assess their capacity to bind ZIKV-susceptible and -permissive cell lines, disrupt ZIKV adsorption, and to interact with dorsal root ganglia (DRG) neurons *ex vivo*. The PRVABC59 sequence was used to generate a peptide that was modified with an NAG molecule at position 8 (equivalent to ASN154), as it natively occurs in this strain, and without carbohydrate modification. ZVBM peptides from MR_766 and PRVABC59 (NAGylated and unglycosylated) all bound Vero cells at levels significantly above those of scrambled PRVABC59 (NAGylated and unglycosylated) controls (Fig. 2A, supplemental Fig. S1), suggesting that this motif has the potential to serve as a ZIKV receptor. Binding of the MR_766 ZVBM peptides, despite a four-amino acid deletion relative to PRVABC59, suggests that the critical portion of the ZVBM is potentially contained entirely on the aminoterminal (NTD) or the carboxyterminal (CTD). A peptide representing the NTD of PRVABC59 was unable to bind Vero cells above scrambled control, whereas a peptide representing the CTD bound significantly ($P<0.05$) above the scrambled control, indicating that the putative receptor is contained entirely on the CTD of ZVBM (Fig. 2B). Pretreatment of Vero cell monolayers with the unglycosylated ("Africanized") PRVABC59 ZVBM significantly ($P<0.01$) inhibited infectivity of ZIKV MR_766; conversely, pretreatment of Vero cells with the NAGylated (native) PRVABC59 ZVBM significantly ($P<0.05$) inhibited infectivity of ZIKV PRVABC59 (Fig. 2C, Supplemental Table S1). These findings demonstrate that adherence of ZVBM peptides to Vero cells has functional relevance, and that this motif mediates at least some host cell adsorption.

Unglycosylated ZVBM peptides from MR_766 and PRVABC59 bound Madin-Darby Canine Kidney (MDCK) cells significantly ($P<0.05$) above (unglycosylated) scrambled control. Interestingly, NAGylated PRVABC59 did not bind MDCK cells above the NAGylated scrambled control, indicating that functionality of ZVBM as a receptor is host cell-specific (Fig. 2D). Given that MDCK cells are still permissive for ZIKV replication⁴⁰, we hypothesized that a more generalized receptor may be contributing to viral adsorption when ZVBM is NAGylated. The association of human AXL with ZIKV adsorption³¹⁻³³ suggests that viral phosphatidyl serine (PS) may facilitate entry into certain host cells by binding Gas6, which in turn binds AXL, as is seen with multiple viruses⁴¹⁻⁴⁵. We pretreated ZIKV strains MR_766 and PRVABC59 with the

PS-binding protein Annexin V prior to infection of Vero cell monolayers. Annexin V significantly ($P<0.05$) inhibited infectivity of PRVABC59 relative to untreated controls (51% reduction) but did not inhibit MR_766 (Fig.2E, Supplemental Table S1), indicating that PS-mediated ZIKV adsorption is possible for ZVBM- NAGylated (*i.e.*, Asian and American lineage) strains. While at least one additional mechanism has been described for the greater infectivity of Asian and American strains³⁷, PS-mediated host cell entry is likely to contribute to this phenotype as well. The capacity of Asian and American lineage strains to utilize at least two binding mechanisms (*i.e.*, PS and ZVBM) suitably explains how AXL can serve as a host cell receptor, but animals who have undergone genetic ablation for *axl* can still serve as permissive hosts for ZIKV⁴⁶⁻⁴⁸.

ZVBM Binding to Neuronal Cells

Disease or infectivity with MR_766 following intrathecal or intracerebral inoculation *in vivo* or neuronal cell infection *in vitro* has been reported⁴⁹⁻⁵³. These findings stand in conflict with a lack of evidence for central nervous system (CNS) involvement during human disease caused by African ZIKV strains. We hypothesized that exposure to neuronal cells *ex vivo* would result in MR_766 ZVBM peptide binding, and the lack of neurological complications during Zika virus disease caused by African strains stems from an inability of these strains to penetrate into the CNS. We collected dorsal root ganglia from C57/black mice and cultured DRG neurons on coverslips. ZVBM peptides from PRVABC59 (unglycosylated), MR_766, and IbH30656 were all shown to bind 24-hour DRG neuron cultures by confocal microscopy (Figure 3A-D). Binding was not detected for the scrambled PRVABC59 control peptide. These findings were consistent with those of Annamalai *et al.*, who demonstrated a lack of neurological disease with strains lacking NAGylation at ASN154 when injected intravenously, and overt disease when the same strain was injected intracranially⁵⁴.

The outcomes of our *in vitro* and *ex vivo* studies suggest a model of ZIKV neurotropism stemming from NAGylation of the ASN154 facilitating entry into the CNS, wherein binding of certain neuronal cells occurs via the carboxyterminal portion of the ZVBM (*i.e.*, ENRAKV). This model is consistent with both the clinical disparity between ZIKV lineages and the generation of neurological disease by the African strain MR_766 when introduced directly into the CNS as previously described^{37, 50}. Our findings also support previous studies that both implicate AXL as a host cell ligand for Asian/American ZIKV strains and those that show genetically ablated animals are still susceptible to infection by establishing two distinct binding mechanisms for this clade^{31-33, 46-48}. These findings demonstrate the impact of NAGylation of a pathogen surface protein in the vicinity of its binding motif; namely, that there is enhanced potential to penetrate into privileged body sites. This change in posttranslational modification can therefore instantly expand the potential target tissues of infectious agents, and can be expected to similarly expand the array of clinical presentations they cause in turn.

Methods

Virus Isolates and Culture Conditions. African Green Monkey Kidney (Vero) cells and Madin-Darby Canine Kidney (MDCK) cells were obtained from the American Type Culture Collection. Cells were routinely propagated in Earle's Minimum Essential Medium (EMEM) with Earle's Balanced Salt Solution, supplemented with 10% fetal bovine serum, L-glutamine and Penicillin/Streptomycin. Cell cultures were incubated at 37°C, with 5% CO₂ and a relative humidity (RH) of 90%. Low-passage isolates of ZIKV strains MR_766 (ATCC VR-84, Uganda) and PRVABC59 (ATCC VR-1843, Puerto Rico) were obtained from the American Type Culture Collection. Virus stocks were propagated on monolayers of Vero cells. Harvested virus lysates were clarified by low-speed centrifugation (500xg/10 min.) and stored in 1-ml aliquots at -80°C.

Protein Analysis and Peptide Design. The Envelope protein structure was visualized using Jmol via the Protein Data Bank (PDB ID 5JHM)⁵⁵⁻⁵⁶, and the PDB Ligand Explorer was used to visualize the structure of N-acetyl glucosamine on ASN154. Probabilities of protein disorder at each amino acid site was estimated using PrDOS⁵⁷. This analysis indicated that the region surrounding ASN154 constitutes a highly disordered linear epitope. Synthetic peptides representing this linear epitope including the differentially glycosylated ASN154 were generated (see Table 1) by Bachem (Bubendorf, Switzerland). The aminoterminal and carboxyterminal domains from PRVABC59 were also synthesized. Peptides were modified by the addition of an aminoterminal FITC label to allow detection and visualization.

Primary Dorsal Root (DRG) Ganglia Neuron Culture. Adult C57/black mice were anesthetized and perfused transcardially with 4°C 1x PBS. Cervical, thoracic and lumbar DRGs were dissected in Ca⁺⁺/Mg⁺⁺-free Hank's basic salt solution (HBSS) and dissociated as previously described⁵⁸. DRGs were cultivated on laminin/polyD-lysine coated EZ slides (MilliporeSigma, Burlington, MA) for 18-24 hours in F-12 medium (Gibco, ThermoFisher Scientific, Waltham, MA) supplemented with 10 % fetal bovine serum, 1 % penicillin/streptomycin at 37° C/5% CO₂. Bound peptides were visualized with a Leica TCS SP5 confocal laser scanning microscope.

Peptide Binding Assays. Vero cells and MDCK cells, both of which are permissive for all Zika strains, were grown to 80% confluency in 48-well plates. Following the removal of medium, wells were blocked with 10% fetal bovine serum for 30 minutes at 37° C. Peptides (100 µg/mL) were incubated with Vero or MDCK cells for 1 hour at 37° C. Unbound peptides were removed by washing with 1x PBS, and mammalian cells were counterstained with DAPI (diluted 1:300) to control for minor variations in monolayer populations. Bound peptides (FITC) were detected at 485/490 (excitation/emission), and cells were quantified at 350/460. Data are presented as FITC:DAPI ratios. Statistical significance was measured by analyses of variance, and by Fisher's Protected Least Significant Difference test for posthoc comparisons when main effects were significant (GraphPad Prism v. 6.0). Primary DRG neurons grown on coverslips were incubated with 100 µg peptide for 1 hour at 37° C. Unbound peptides were removed by washing with HBSS, and DRG neurons were counterstained with DAPI (diluted 1:300). Bound peptides were visualized using Keyence BZX-700 inverted widefield digital microscope.

178

179 *Viral Adsorption Inhibition Assays by ZVBM Peptides.* Vero cells were propagated in 48-well plates (seed
180 concentration-1e5 cells/well) for 24-hr. Resulting monolayers (85% confluence) were washed twice with
181 warmed PBS and incubated for 2 hours (37° C, 5% CO₂, 90% RH) with 0.1 ml volumes of either PBS
182 (Negative Control), or PBS containing 467 ug of the selected ZVBM peptide. Following treatment, PBS or
183 peptide was decanted, and monolayers washed twice with warmed PBS. ZIKV stocks (stock
184 concentrations: Strain MR_766 – 3.16 e7 TCID₅₀/ml; Strain PRVABC59 – 2e7 TCID₅₀/ml) were serially
185 diluted in serum-free Dulbecco's Minimum Essential Medium (DMEM). Host cell monolayers in treated,
186 or untreated plates were inoculated with either strain MR_766 or PRVABC59 (0.1 ml/well, 5 wells per
187 dilution, N = 3 replicates each) and incubated for 2 hr. After inocula were removed, wells were
188 supplemented with 0.5 ml EMEM growth medium and returned to the incubator. Virus cytopathogenic
189 effects (CPE) were monitored and scored over a period of 10-12 days and the resulting virus titers
190 calculated as TCID₅₀/ml. Statistical significance of changes in virus titer as a result of peptide
191 pretreatment versus untreated control was measured by *Student's* T- test (GraphPad Prism v. 6.0).

192

193 *Virus Treatment with Annexin V.* Annexin V (AbCam, Cambridge, MA) was dissolved in PBS (2335 ug/ml)
194 and filter-sterilized (0.2 um). ZIKV stocks MR_766 and PRVABC59 were then serially diluted in either
195 PBS, or PBS-Annexin V. Dilutions were incubated for 2 hours (37° C, 5% CO₂, 90% RH). Host cell
196 monolayers, prepared in 48-well plates as previously described, were inoculated with respective virus
197 dilutions (0.1 ml/well, 5 wells per dilution, N = 3 replicates each). Virus CPE were scored over a period of
198 10-12 days and the resulting virus titers calculated as TCID₅₀/ml. Statistical significance of changes in
199 virus titer as a result of Annexin V pretreatment versus untreated control was measured by *student's* T
200 test (GraphPad Prism v. 6.0) for each ZIKV strain.

201

202 *Ethical Assurance Statements.* All methods were carried out in accordance with relevant
203 guidelines and regulations. Collection of DRG neurons was performed in accordance with a
204 protocol approved by the University of New England's Institutional Animal Care and Use
205 Committee.

206

207 **Acknowledgements:** This work was supported by intramural awards from the University of New England
208 Center of Excellence for Neuroscience (CEN) an the Office of the Vice President for Research and
209 Scholarship. The authors wish to thank Peter Caradonna (CEN Histology and Imaging Core), Denise
210 Giuvelis (CEN Behavioral Core), and Joshua Havelin for their assistance.

211

212 **Author Contributions:** Peptide motif design and experimentation (CAR, JR, SS); structural and
213 informatics analysis (MM, RFR); neuronal cell extraction development, binding experimentation,

confocal imaging parameters (DG, RG, DCM, CAR, SS); viral replication inhibition studies (JV, CAR); Study design, management, execution, and data analysis (MM, RFR, TEK); manuscript preparation (CAR, MM)

Additional Information:

Competing interests

The authors declare no competing interests.

References

1. Sampathkumar, P. & Sanchez, J. L. Zika Virus in the Americas: A Review for Clinicians. *Mayo Clin. Proc.* **91** 514-21 (2016).
2. Wikan, N. & Smith, D. R. Zika virus: history of a newly emerging arbovirus. *Lancet Infect. Dis.* **16** e119-e126, (2016).
3. Besnard, M., Lastere, S., Teissier, A., Cao-Lormeau, V., & Musso, D. Evidence of perinatal transmission of Zika virus, French Polynesia, December 2013 and February 2014. *Euro. Surveill.* **19**, (2014).
4. Cauchemez, S., Besnard, M., Bompard, P., Dub, T., Guillemette-Artur, P., Eyrolle-Guignot, D., Salje, H., Van Kerkhove, M. D., Abadie, V., Garel, C., Fontanet, A., & Mallet, H. P. Association between Zika virus and microcephaly in French Polynesia, 2013-15: a retrospective study. *Lancet* **387** 2125-2132, (2016).
5. Brasil, P., Calvet, G. A., Siqueira, A. M., Wakimoto, M., de Sequeira, P. C., Nobre, A., Quintana, M. e. S., Mendonça, M. C., Lupi, O., de Souza, R. V., Romero, C., Zogbi, H., Bressan, C. a. S., Alves, S. S., Lourenço-de-Oliveira, R., Nogueira, R. M., Carvalho, M. S., de Filippis, & A. M., Jaenisch, T. Zika Virus Outbreak in Rio de Janeiro, Brazil: Clinical Characterization, Epidemiological and Virological Aspects. *PLoS Negl. Trop. Dis.* **10** e0004636, (2016).
6. Brasil, P., Sequeira, P. C., Freitas, A. D., Zogbi, H. E., Calvet, G. A., de Souza, R. V., Siqueira, A. M., de Mendonca, M. C., Nogueira, R. M., de Filippis, A. M., & Solomon, T. Guillain-Barré syndrome associated with Zika virus infection. *Lancet* **387** 1482, (2016).
7. Rasmussen, S. A., Jamieson, D. J., Honein, M. A., & Petersen, L. R. Zika Virus and Birth Defects - Reviewing the Evidence for Causality. *N. Engl. J. Med.* **374** 1981-7, (2016).
8. de Fatima Vasco Aragao, M., van der Linden, V., Brainer-Lima, A. M., Coeli, R. R., Rocha, M. A., Sobral da Silva, P., Durce Costa Gomes de Carvalho, M., van der Linden, A., Cesario de Holanda, A., & Valenca, M. M. Clinical features and neuroimaging (CT and MRI) findings in presumed Zika virus related congenital infection and microcephaly: retrospective case series study. *BMJ* **353** i1901, (2016).
9. Mehrjardi, M. Z. Is Zika Virus an Emerging TORCH Agent? An Invited Commentary. *Virology (Auckl)* **8** 1178122X17708993, (2017).
10. Melo, A. S., Aguiar, R. S., Amorim, M. M., Arruda, M. B., Melo, F. O., Ribeiro, S. T., Batista, A. G., Ferreira, T., Dos Santos, M. P., Sampaio, V. V., Moura, S. R., Rabello, L. P., Gonzaga, C. E., Malinger,

- G., Ximenes, R., de Oliveira-Szejnfeld, P. S., Tovar-Moll, F., Chimelli, L., Silveira, P. P., Delvechio, R., Higa, L., Campanati, L., Nogueira, R. M., Filippis, A. M., Szejnfeld, J., Voloch, C. M., Ferreira, O. C., Brindeiro, R. M., & Tanuri, A. Congenital Zika Virus Infection: Beyond Neonatal Microcephaly. *JAMA Neurol.* **73** 1407-1416, (2016).
11. Mlakar, J., Korva, M., Tul, N., Popović, M., Poljšak-Prijatelj, M., Mraz, J., Kolenc, M., Resman Rus, K., Vesnaver Vipotnik, T., Fabjan Vodusek, V., Vizjak, A., Pižem, J., Petrovec, M., & Avšič Županc, T. Zika Virus Associated with Microcephaly. *N. Engl. J. Med.* **374** 951-8, (2016).
12. Reynolds, M. R., Jones, A. M., Petersen, E. E., Lee, E. H., Rice, M. E., Bingham, A., Ellington, S. R., Evert, N., Reagan-Steiner, S., Oduyebo, T., Brown, C. M., Martin, S., Ahmad, N., Bhatnagar, J., Macdonald, J., Gould, C., Fine, A. D., Polen, K. D., Lake-Burger, H., Hillard, C. L., Hall, N., Yazdy, M. M., Slaughter, K., Sommer, J. N., Adamski, A., Raycraft, M., Fleck-Derderian, S., Gupta, J., Newsome, K., Baez-Santiago, M., Slavinski, S., White, J. L., Moore, C. A., Shapiro-Mendoza, C. K., Petersen, L., Boyle, C., Jamieson, D. J., Meaney-Delman, D., & Honein, M. A., Collaboration, U. S. Z. P. R. Vital Signs: Update on Zika Virus-Associated Birth Defects and Evaluation of All U.S. Infants with Congenital Zika Virus Exposure - U.S. Zika Pregnancy Registry, 2016. *MMWR Morb. Mortal. Wkly. Rep.* **66** 366-373, (2017).
13. Acevedo, N., Waggoner, J., Rodriguez, M., Rivera, L., Landivar, J., Pinsky, B., & Zambrano, H. Zika Virus, Chikungunya Virus, and Dengue Virus in Cerebrospinal Fluid from Adults with Neurological Manifestations, Guayaquil, Ecuador. *Front. Microbiol.* **8** doi: 10.3389/fmicb.2017.00042. eCollection 2017 (2017).
14. De Broucker, T., Mailles, A., & Stahl, J. P. Neurological Presentation of Zika Virus Infection Beyond the Perinatal Period. *Curr. Infect. Dis. Rep.* **19** 35 (2017).
15. Dub, T. & Fontanet, A. Zika virus and Guillain-Barré syndrome. *Rev. Neuro.l (Paris)* **173** 361-363 (2017).
16. Galliez, R. M., Spitz, M., Rafful, P. P., Cagy, M., Escosteguy, C., Germano, C. S., Sasse, E., Gonçalves, A. L., Silveira, P. P., Pezzuto, P., Ornelas, A. M., Tanuri, A., Aguiar, R. S., & Moll, F. T. Zika Virus Causing Encephalomyelitis Associated With Immunoactivation. *Open Forum Infect. Dis.* **3** ofw203, (2016).
17. Roth, W., Tyshkov, C., Thakur, K., & Vargas, W. Encephalomyelitis Following Definitive Zika Virus Infection. *Neurol Neuroimmunol Neuroinflamm* **4** e349, (2017).
18. Rozé, B., Najioullah, F., Signate, A., Apetse, K., Brouste, Y., Gourgoudou, S., Fagour, L., Abel, S., Hochedez, P., Cesaire, R., Cabié, A., & the Martinique Neuro-Zika Working Group. Zika virus detection in cerebrospinal fluid from two patients with encephalopathy, Martinique, February 2016. *Euro. Surveill.* **21** doi: 10.2807/1560-7917.ES.2016.21.16.30205, (2016).
19. Thiery, G., Valentino, R., & Meddhaoui, H. Zika virus-associated Guillain-Barré syndrome: a warning for critical care physicians. *Intensive Care Med.* **42** 1485-6, (2016).
20. Zare Mehrjardi, M., Keshavarz, E., Poretti, A., Hazin, A. N. Neuroimaging findings of Zika virus infection: a review article. *Jpn J Radiol* **34** 765-770 (2016).
21. Rosenberg, A. Z., Yu, W., Hill, D. A., Reyes, C. A., & Schwartz, D. A. Placental Pathology of Zika Virus: Viral Infection of the Placenta Induces Villous Stromal Macrophage (Hofbauer Cell) Proliferation and Hyperplasia. *Arch. Pathol. Lab Med.* **141** 43-48, (2017).

22. Ma, W., Li, S., Ma, S., Jia, L., Zhang, F., Zhang, Y., Zhang, J., Wong, G., Zhang, S., Lu, X., Liu, M., Yan, J., Li, W., Qin, C., Han, D., Wang, N., Li, X., & Gao, G. F. Zika Virus Causes Testis Damage and Leads to Male Infertility in Mice. *Cell* **167** 1511-1524.e10, (2016).
23. Jogueux, G., Mansuy, J. M., Matusali, G., Hamdi, S., Walschaerts, M., Pavili, L., Guyomard, S., Prisant, N., Lamarre, P., Dejucq-Rainsford, N., Pasquier, C., & Bujan, L. Effect of acute Zika virus infection on sperm and virus clearance in body fluids: a prospective observational study. *Lancet Infect. Dis.* **17** 1200-1208 (2017).
24. Brent, C., Dunn, A., Savage, H., Faraji, A., Rubin, M., Risk, I., Garcia, W., Cortese, M., Novosad, S., Krow-Lucal, E. R., Crain, J., Hill, M., Atkinson, A., Peterson, D., Christensen, K., Dimond, M., Staples, J. E., & Nakashima, A. Preliminary Findings from an Investigation of Zika Virus Infection in a Patient with No Known Risk Factors - Utah, 2016. *MMWR Morb. Mortal. Wkly. Rep.* **65** 981-2, (2016).
25. Zonneveld, R., Roosblad, J., Staveren, J. W., Wilschut, J. C., Vreden, S. G., & Codrington, J. Three atypical lethal cases associated with acute Zika virus infection in Suriname. *ID Cases* **5** 49-53 (2016).
26. Relich, R. F. & Loeffelholz, M. Zika Virus. *Clin Lab Med* **37** 253-267, (2017).
27. May, M. & Relich, R. F. A Comprehensive Systems Biology Approach to Studying Zika Virus. *PLoS One* **11** e0161355, (2016).
28. Faye, O., Freire, C. C., Iamarino, A., de Oliveira, J. V., Diallo, M., Zanotto, P. M., & Sall, A. A. Molecular evolution of Zika virus during its emergence in the 20(th) century. *PLoS Negl. Trop. Dis.* **8** e2636, (2014).
29. Lanciotti, R. S., Lambert, A. J., Holodniy, M., Saavedra, S., & Signor, L. e. C. Phylogeny of Zika Virus in Western Hemisphere, 2015. *Emerg. Infect. Dis.* **22** 933-5, (2016).
30. Zhu, Z., Chan, J. F., Tee, K. M., Choi, G. K., Lau, S. K., Woo, P. C., Tse, H., & Yuen, K. Y. Comparative genomic analysis of pre-epidemic and epidemic Zika virus strains for virological factors potentially associated with the rapidly expanding epidemic. *Emerg. Microbes Infect.* **5** e22, (2016).
31. Liu, S., DeLalio, L. J., Isakson, B. E., & Wang, T. T. AXL-Mediated Productive Infection of Human Endothelial Cells by Zika Virus. *Circ. Res.* **119** 1183-1189, (2016).
32. Nowakowski, T. J., Pollen, A. A., Di Lullo, E., Sandoval-Espinosa, C., Bershteyn, M., & Kriegstein, A. R. Expression Analysis Highlights AXL as a Candidate Zika Virus Entry Receptor in Neural Stem Cells. *Cell Stem Cell* **18** 591-6 (2016).
33. Richard, A. S., Shim, B. S., Kwon, Y. C., Zhang, R., Otsuka, Y., Schmitt, K., Berri, F., Diamond, M. S., & Choe, H. AXL-dependent infection of human fetal endothelial cells distinguishes Zika virus from other pathogenic flaviviruses. *Proc. Natl. Acad. Sci. USA* **114** 2024-2029, (2017).
34. Bardina, S. V., Bunduc, P., Tripathi, S., Duehr, J., Frere, J. J., Brown, J. A., Nachbagauer, R., Foster, G. A., Kryzstof, D., Tortorella, D., Stramer, S. L., Garcia-Sastre, A., Krammer, F., & Lim, J. K. Enhancement of Zika virus pathogenesis by preexisting ant flavivirus immunity. *Science* **356**, 175-180 (2017).
35. Castanha, P. M. S., Nascimento, E. J. M., Braga, C., Cordeiro, M. T., de Carvalho, O. V., de Mendonça, L. R., Azevedo, E. A. N., França, R. F. O., Dhalia, R., & Marques, E. T. A. Dengue Virus-Specific Antibodies Enhance Brazilian Zika Virus Infection. *J. Infect. Dis.* **215** 781-785, (2017).
36. Paul, L. M., Carlin, E. R., Jenkins, M. M., Tan, A. L., Barcello, C. M., Nicholson, C. O., Michael, S. F., & Isern, S. Dengue virus antibodies enhance Zika virus infection. *Clin. Transl. Immunology* **5** e117, (2016).

37. Yuan, L., Huang, X. Y., Liu, Z. Y., Zhang, F., Zhu, X. L., Yu, J. Y., Ji, X., Xu, Y. P., Li, G., Li, C., Wang, H. J., Deng, Y. Q., Wu, M., Cheng, M. L., Ye, Q., Xie, D. Y., Li, X. F., Wang, X., Shi, W., Hu, B., Shi, P. Y., Xu, Z., & Qin, C. F. A single mutation in the prM protein of Zika virus contributes to fetal microcephaly. *Science* **358** 933-936 (2017).
38. Dowall, S. D., Graham, V. A., Rayner, E., Atkinson, B., Hall, G., Watson, R. J., Bosworth, A., Bonney, L. C., Kitchen, S., & Hewson, R. A Susceptible Mouse Model for Zika Virus Infection. *PLoS Negl. Trop. Dis.* **10** e0004658, (2016).
39. Koide, F., Goebel, S., Snyder, B., Walters, K. B., Gast, A., Hagelin, K., Kalkeri, R., & Rayner, J. Development of a Zika Virus Infection Model in Cynomolgus Macaques. *Front. Microbiol.* **7** 2028 (2016).
40. Barr, K. L., Anderson, B. D., Prakoso, D., Long, M. T. Working with Zika and Usutu Viruses In Vitro. *PLoS Negl. Trop. Dis.* **10** e0004931, (2016).
41. Carnec, X., Meertens, L., Dejarnac, O., Perera-Lecoin, M., Hafirassou, M. L., Kitauro, J., Ramdasi, R., Schwartz, O., & Amara, A. The Phosphatidylserine and Phosphatidylethanolamine Receptor CD300a Binds Dengue Virus and Enhances Infection. *J. Virol.* **90** 92-102, (2015).
42. Jemielity, S., Wang, J. J., Chan, Y. K., Ahmed, A. A., Li, W., Monahan, S., Bu, X., Farzan, M., Freeman, G. J., Umetsu, D. T., Dekruyff, R. H., & Choe, H. TIM-family proteins promote infection of multiple enveloped viruses through virion-associated phosphatidylserine. *PLoS Pathog.* **9** e1003232 (2013).
43. Meertens, L., Labeau, A., Dejarnac, O., Cipriani, S., Sinigaglia, L., Bonnet-Madin, L., Le Charpentier, T., Hafirassou, M. L., Zamborlini, A., Cao-Lormeau, V. M., Couplier, M., Missé, D., Jouvenet, N., Tabibiazar, R., Gressens, P., Schwartz, O., & Amara, A. Axl Mediates ZIKA Virus Entry in Human Glial Cells and Modulates Innate Immune Responses. *Cell Rep.* **18** 324-333, (2017).
44. Richard, A. S., Zhang, A., Park, S. J., Farzan, M., Zong, M., & Choe, H. Virion-associated phosphatidylethanolamine promotes TIM1-mediated infection by Ebola, dengue, and West Nile viruses. *Proc. Natl. Acad. Sci. USA* **112** 14682-7 (2015).
45. Wang, J., Qiao, L., Hou, Z., & Luo, G. TIM-1 Promotes Hepatitis C Virus Cell Attachment and Infection. *J. Virol.* **91** e01583-16, (2017).
46. Hastings, A. K., Yockey, L. J., Jagger, B. W., Hwang, J., Uraki, R., Gaitsch, H. F., Parnell, L. A., Cao, B., Mysorekar, I. U., Rothlin, C. V., Fikrig, E., Diamond, M. S., & Iwasaki, A. TAM Receptors Are Not Required for Zika Virus Infection in Mice. *Cell Rep.* **19** 558-568, (2017).
47. Li, F., Wang, P. R., Qu, L. B., Yi, C. H., Zhang, F. C., Tang, X. P., Zhang, L. G., & Chen, L. AXL is not essential for Zika virus infection in the mouse brain. *Emerg. Microbes Infect.* **6** e16, (2017).
48. Wells, M. F., Salick, M. R., Wiskow, O., Ho, D. J., Worringer, K. A., Ihry, R. J., Kommineni, S., Bilican, B., Klim, J. R., Hill, E. J., Kane, L. T., Ye, C., Kaykas, A., & Egan, K. Genetic Ablation of AXL Does Not Protect Human Neural Progenitor Cells and Cerebral Organoids from Zika Virus Infection. *Cell Stem Cell* **19** 703-708, (2016).
49. Duggal, N. K., Ritter, J. M., McDonald, E. M., Romo, H., Guirakhoo, F., Davis, B. S., Chang, G. J., & Brault, A. C. Differential Neurovirulence of African and Asian Genotype Zika Virus Isolates in Outbred Immunocompetent Mice. *Am. J. Trop. Med. Hyg.* **97** 1410-1417, (2017).
50. Li, C., Xu, D., Ye, Q., Hong, S., Jiang, Y., Liu, X., Zhang, N., Shi, L., Qin, C. F., & Xu, Z. Zika Virus Disrupts Neural Progenitor Development and Leads to Microcephaly in Mice. *Cell Stem Cell* **19** 120-6 (2016).

51. Shao, Q., Herrlinger, S., Yang, S. L., Lai, F., Moore, J. M., Brindley, M. A., & Chen, J. F. Zika virus infection disrupts neurovascular development and results in postnatal microcephaly with brain damage. *Development* **143** 4127-4136, (2016).
52. Shao, Q., Herrlinger, S., Zhu, Y. N., Yang, M., Goodfellow, F., Stice, S. L., Qi, X. P., Brindley, M. A., & Chen, J. F. The African Zika virus MR-766 is more virulent and causes more severe brain damage than current Asian lineage and dengue virus. *Development* **144** 4114-4124, (2017).
53. Tang, H., Hammack, C., Ogden, S. C., Wen, Z., Qian, X., Li, Y., Yao, B., Shin, J., Zhang, F., Lee, E. M., Christian, K. M., Didier, R. A., Jin, P., Song, H., & Ming, G. L. Zika Virus Infects Human Cortical Neural Progenitors and Attenuates Their Growth. *Cell Stem Cell* **18** 587-90, (2016).
54. Annamalai, A. S., Pattnaik, A., Sahoo, B. R., Muthukrishnan, E., Natarajan, S. K., Steffen, D., Vu, H. L. X., Delhon, G., Osorio, F. A., Petro, T. M., Xiang, S. H., & Pattnaik, A. K. Zika Virus Encoding Non-Glycosylated Envelope Protein is Attenuated and Defective in Neuroinvasion. *J. Virol.* doi: 10.1128/JVI.01348-17. (2017).
55. Berman, H. M., Bhat, T. N., Bourne, P. E., Feng, Z., Gilliland, G., Weissig, H., & Westbrook, J. The Protein Data Bank and the challenge of structural genomics. *Nat. Struct. Biol.* **7**, 957-9 (2000).
56. Dai, L., Song, J., Lu, X., Deng, Y. Q., Musyoki, A. M., Cheng, H., Zhang, Y., Yuan, Y., Song, H., Haywood, J., Xiao, H., Yan, J., Shi, Y., Qin, C. F., Qi, J., & Gao, G. F. Structures of the Zika Virus Envelope Protein and Its Complex with a Flavivirus Broadly Protective Antibody. *Cell Host Microbe* **19** 696-704, (2016).
57. Ishida, T. & Kinoshita, K. PrDOS: prediction of disordered protein regions from amino acid sequence. *Nucleic Acids Res.* **35** W460-4, (2007).
58. Malin, S. A., Davis, B. M., Molliver, D. C. Production of dissociated sensory neuron cultures and considerations for their use in studying neuronal function and plasticity. *Nat. Protoc.* **2** 152-60, (2007).

Table 1: Peptide Sequences

Peptide Name ^a	Sequence ^b	Strain Type ^c
PRVABC59-N	*QHSGMIVNDTGHETDENRAKV	Asian/American
PRVABC59	*QHSGMIVNDTGHETDENRAKV	“African”
MR_766	*QHSGMI----GYETDENRAKV	African
IbH30656	*QHSGMIVND-----ENRAKV	African
Scrambled	*QDHVIHVDMTGRTGSEEANKN	N/A
Scrambled-N	*QDHVIHVDMTGRTGSEEANKN	N/A
PRVABC59-NTD	*QHSGMIVND	“African” partial
PRVABC59-CTD	*ENRAKV	Asian/American

^aPeptides are named for the strain they derived from. The modifiers N, NTD, and CTD reflect the addition of NAG, use of the aminoterminal domain, or the carboxyterminal domain, respectively.

^bAsterisk (*) indicate location of the FITC molecule. Shaded asparagine (N) residues indicate location of NAG coupling.

^cThe designation “African” indicates that sequence from the Asian/American clade strain PRVABC59 has been made to resemble an African strain by its lack of NAG.

Figures and Figure Legends

Figure 1: Envelope Protein Structure. (A) The predicted E protein structure indicates that the region containing ASN154 (circled) and its NAG modification (inset) is a linear β strand. Intrinsic disorder probabilities were calculated for each amino acid position in the E protein sequence from strains (B) PRVABC59, (C) MR_766, and (D) IbH30656. Probabilities above 0.5 (blue line) are considered indicative of sites representing disordered regions. The region containing ASN154 is indicated (blue box) for each strain.

Figure 2: ZVBM Binding and ZIKV Inhibition. (A) NAGylated or unglycosylated ZVBM peptides from strain PRVABC59 and the type strain MR_766 bound Vero cells significantly (* $P < 0.05$) above scrambled ZVBM sequences from PRVABC59, with or without NAG modification. (B) A shorter peptide representing the NTD of PRVABC59 was unable to bind Vero cells above the full-length ZVBM scrambled control; however, a peptide representing the CTD bound Vero cells at a significantly (** $P < 0.01$) higher level than the NTD or scrambled control. (C) Pretreatment of Vero cells with unglycosylated ZVBM peptide (PRVABC59) significantly (* $P < 0.05$) inhibited ZIKV MR_766 replication relative to untreated controls, whereas the unglycosylated scrambled control peptide was not. Similarly, pretreatment with NAGylated ZVBM peptide (PRVABC59) significantly (** $P < 0.01$) inhibited ZIKV PRVABC59 replication relative to untreated controls, whereas the NAGylated scrambled control peptide was not. (D) Unglycosylated PRVABC59 and MR_766 ZVBM peptides bound MDCK cells significantly (* $P < 0.05$) above unglycosylated or NAGylated scrambled controls; however, the NAGylated PRVABC59 ZVBM peptide was not. (E) Pretreatment of ZIKV strain PRVABC59 with annexin V significantly (** $P < 0.01$) inhibited viral replication on Vero cells relative to untreated controls, whereas replication of ZIKV MR_766 following pretreatment with annexin V was unaffected.

Figure 3: Peptide binding to DRG Neurons *ex vivo*. Primary DRG neurons from C57 black mice (DAPI, blue fluorescence) were exposed to ZVBM peptides (FITC, green fluorescence) from (A) PRVABC59, (B) MR_766, (C) IbH30656, and (D) PRVABC59 (scrambled). Punctate green staining around the DRG nuclei was observed via laser confocal microscopy in panels A, B, and C, but was largely absent from panel D.

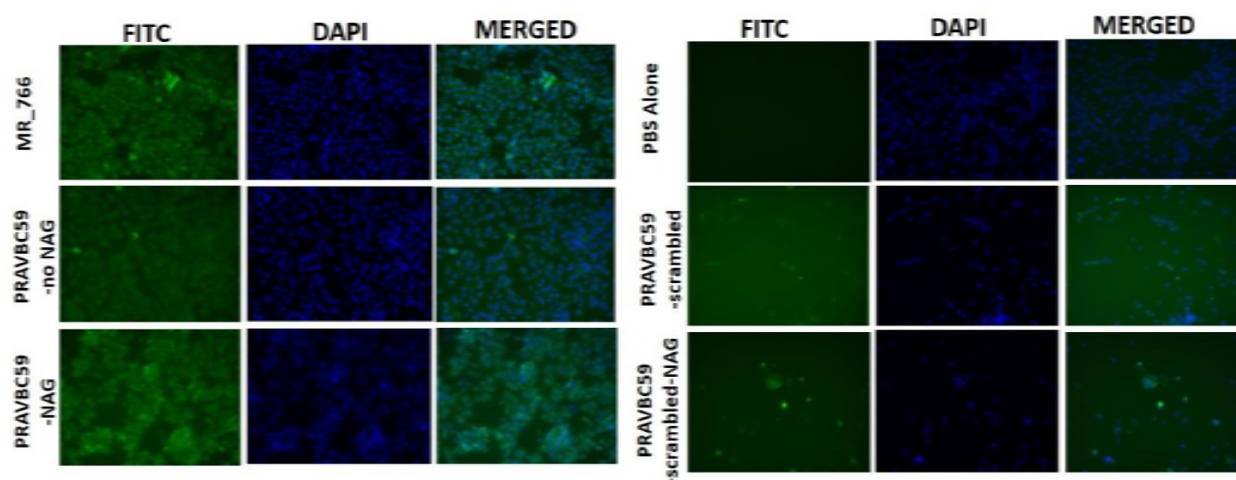
Supplemental Material:

Supplemental Table S1: ZIKV Adsorption Inhibition

Strain/Treatment	Mean TCID ₅₀	Significant Reduction?
ZIKV MR_766	9136667 ± 61191.3	--

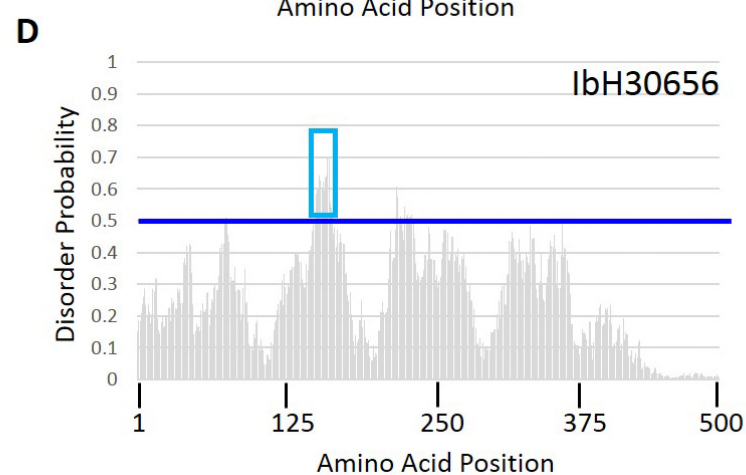
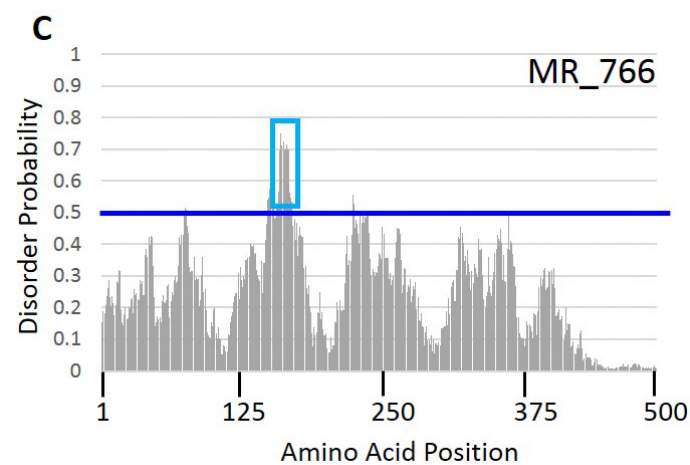
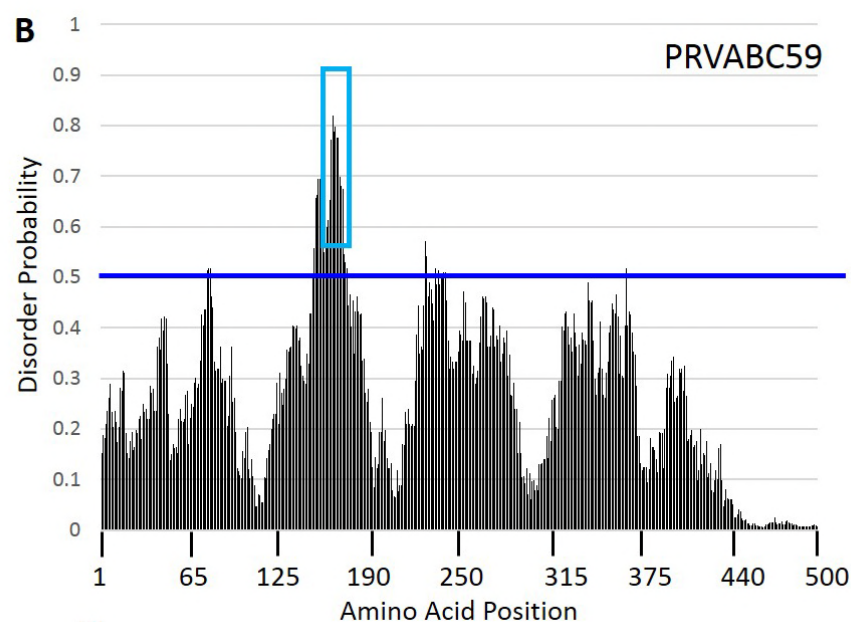
ZIKV MR_766 + PRVABC59 ZVBM (no NAG)	1470000 ± 1895.2	Yes ($P<0.05$)
ZIKV MR_766	1085333 ± 66626.2	--
ZIKV MR_766 + PRVABC59 ZVBM (no NAG) - Scrambled	1288667 ± 89581.3	No
ZIKV PRVABC59	1920500 ± 1752918	--
ZIKV PRVABC59 + PRVABC59 ZVBM (NAG)	893666.7 ± 184175	Yes ($P<0.01$)
ZIKV PRVABC59	1470000 ± 2264	--
ZIKV PRVABC59 + PRVABC59 ZVBM (NAG) - Scrambled	473000 ± 18776	No
ZIKV PRVABC59	177033.3 ± 43766.67	--
ZIKV PRVABC59 + Annexin V	43766.67 ± 21073.28	Yes ($P<0.01$)
ZIKV MR_766	164866.7 ± 143039.3	--
ZIKV MR_766 + Annexin V	197366.7 ± 126649.5	No

456

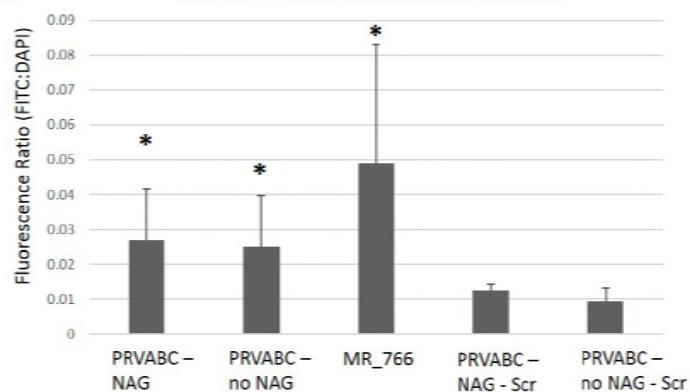


457

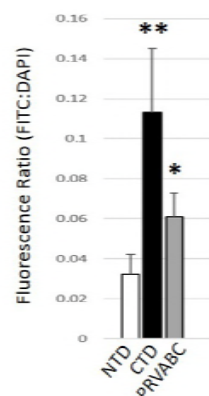
458 **Supplemental Figure S1: Peptide binding to Vero Cells.** Vero cell monolayers (85% confluency) (DAPI,
459 blue fluorescence) were exposed to ZVBM peptides (FITC, green fluorescence) from PRVABC59
460 (NAGylated and unglycosylated), MR_766, and scrambled PRVABC59 peptides (NAGylated and
461 unglycosylated). Co-localization of FITC and DAPI staining was observed for glycosylated and
462 unglycosylated PRVABC59 and MR_766 peptides, but was largely absent from scrambled control
463 peptides.



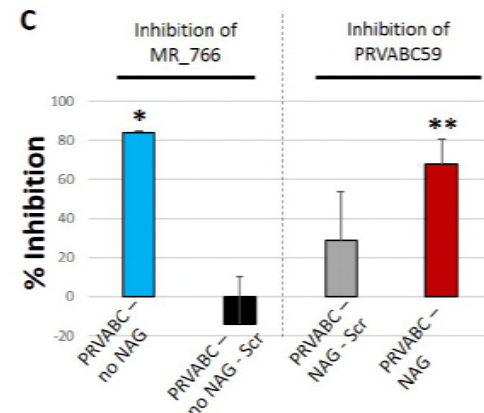
A ZVBM – Vero Cell Interactions



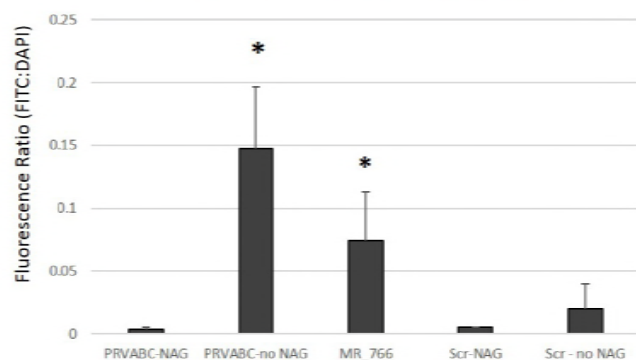
B



C



D ZVBM - MDCK Cell Interactions



E

Annexin V Inhibition of ZIKV

